

High-speed, all-optical XOR gates using semiconductor optical amplifiers in ultrafast nonlinear interferometers

Xuelin YANG (✉)^{1,2}, Qiwei WENG¹, Weisheng HU¹

¹ The State Key Laboratory of Advanced Optical Communication Systems and Networks, Shanghai Jiao Tong University, Shanghai 200240, China
² Photonic Systems Group, Tyndall National Institute, University College Cork, Cork, Ireland

© Higher Education Press and Springer-Verlag Berlin Heidelberg 2010

Abstract We will review three recently-proposed high-speed, all-optical Exclusive OR (XOR) gates operating at 40 and 85 Gb/s, which were demonstrated using ultrafast nonlinear interferometers (UNIs) incorporating semiconductor optical amplifiers (SOAs). The first 40-Gb/s XOR gate was obtained using a dual UNI configuration. The second is a 40-Gb/s XOR gate without additional probe beam required, where the only inputs launched into the setup were data A and B. The XOR logic of data A and B is the sum of two components $\overline{A}B$ and $A\overline{B}$, each of which was obtained from the output of UNI via cross-phase modulation (XPM) in SOAs. Furthermore, an 85-Gb/s XOR gate is, by far, the fastest XOR gate realized by SOAs, which was also demonstrated using a dual UNI structure. The operating speed of the XOR gate was enhanced by incorporating the recently proposed turbo-switch configuration. In addition, the SOA switching pulse energies of these XOR gates were lower than 100 fJ.

Keywords semiconductor optical amplifiers, all-optical logic, Exclusive OR (XOR) gates, high-speed switching

1 Introduction

All-optical binary logic gates such as AND, Exclusive OR (XOR) are expected to become key elements in digital signal processing and optical fiber networks in high bit-rate telecommunication systems [1,2]. Efforts to realize various all-optical binary logic functions have been increasing recently in order to avoid difficulties and costs by using optical-electrical-optical (O-E-O) conversions and, therefore, facilitate the network management and reduce energy consumption. All-optical logic gates such as NOT, AND,

OR, and XOR have been successfully demonstrated by employing gain/phase nonlinearity in semiconductor optical amplifiers (SOAs) [1–5]. The SOAs are very competitive due to their nonlinear gain/phase characteristics, such as the high nonlinearity, low switching power, wide gain bandwidth, compact size, and potential integration capability with other photonic devices. All-optical XOR logic is regarded as one of the fundamental logic gates in signal processing, which plays an important role in applications such as bit pattern recognition [3], pseudo-random bit sequence (PRBS) generation, parity checking and optical computing. A high-speed all-optical XOR gate has potential applications for on-the-fly digital serial processing of optical signals, for example, in packet header recognition, error detection and coding/decoding. In addition, the XOR function has been used recently as a wavelength converter and regenerator for signals in a differential phase shift keying (DPSK) format [6,7].

All-optical 10-Gb/s XOR gates using SOAs were reported using cross-gain modulation (XGM) [5], where the operation speed is limited by the relatively slow carrier recovery time of SOA, typically in an order of 100 ps. Interferometric configurations using cross-phase modulation (XPM) were explored to realize all-optical AND logic at a higher bit rate, such as ultrafast nonlinear interferometer (UNI) [4], delayed interferometer [8] and push-pull configuration [9–11]. These techniques are commonly referred to differential switching methods, which allow the operation speed at bit rates higher than the SOA gain recovery limit. All-optical XOR gate at 40 Gb/s has been achieved by a push-pull scheme in a Mach-Zehnder interferometer (MZI) [12], which was working in a differential mode, and was effectively switched at twice the line rate.

In this paper, we will review three recently-demonstrated all-optical XOR gates incorporating UNI configuration. The new XOR gates consisted of dual cascaded UNI elements, where SOAs were switched at

only the line rate, allowing the potential for a higher ultimate operation speed. The first XOR gate we will report here is a 40-Gb/s gate based on dual cascaded UNI elements [13,14].

The second gate we will report here is a 40-Gb/s XOR without probe beam [15]. All the previously-reported XOR gates have to implement an additional continuous wave (CW) or a pulse clock source with a different wavelength other than the data A and B as a probe beam, which increases the cost and complexity of the XOR gate. A simple XOR logic was first reported in Ref. [5], where only the data sequences A and B are required as input; however, due to the fact that XGM and counter-propagating control data stream configurations were employed in Ref. [5], the XOR gate operation was reported only at 10 Gb/s. In this paper, we will show a 40-Gb/s all-optical XOR gate without any additional probe beam, which is achieved by a UNI structure using the XPM scheme. Besides the improvement of XOR gate operation speed up to 40 Gb/s, the XOR gate also has other advantages such as lower switching power, reduced chirp and enhanced extinction ratio (ER), which is inherently related to SOA-based XPM schemes [8–10].

The third XOR is an improved version of the first XOR gate; however, it can be operated at 85 Gb/s [16]. The high-speed operation of the 85-Gb/s gate was achieved by incorporating the turbo-switch configuration [17] into a dual UNI structure. All-optical 85-Gb/s XOR operation is demonstrated by a clear open-eye diagram. The operating speed is, by far, the fastest SOA-based XOR gate, though the same speed was obtained in Bell Laboratories very recently using a pair of MZI structures [18].

2 Operation principle

SOA-based UNI is a versatile optical switching element using XPM [4], as shown in Fig. 1. In the XPM scheme, when a strong control data pulse is injected into an SOA, it will introduce an intensity-dependent refractive index change in the active layer of the SOA; therefore, a phase shift will be experienced by a following co-propagating

relatively weak probe pulse via XPM due to the carrier dynamics in the SOA. In Fig. 1, two birefringent fibers are used to split and recombine the transverse electric (TE) and transverse magnetic (TM) components of the probe pulse by setting the relative optical delays between TE and TM. A polarizer is used to form an interferometer for the TE and TM beams. In the case the control pulse is not present, the phases experienced by the TE and TM components of the probe pulse in the SOA are the same; therefore, the output signal is matched in phase and maximized after the polarizer (case “1”). On the contrary, in the case the control pulse is launched between the delay time of TE and TM components, due to the carrier depletion by the control pulse, the following TE component will experience a phase shift (for instance, π) compared with the preceding TM component of the probe pulse; therefore, after the TE and TM components recombine and interfere at the polarizer (POL), the output signal is minimized due to the π phase shift between TE and TM components (case “0”), as shown in Fig. 1. This results in AND gate operation.

To realize the XOR gate function, two UNI elements are cascaded to allow the two data pulse streams A and B to be input into SOA1 and SOA2, respectively, as control pulses. The scheme of the XOR logic gate is shown in Fig. 2. The input probe pulses are launched into a polarization maintaining (PM) fiber with equal intensities on the fast and slow fiber axes, which are coupled to the TM and TE axes of SOA1, respectively. As a result, the TE pulse lags the TM pulse by Δt . The control pulse A is introduced between the two probe pulse components before they are input in SOA1, in which it induces a π radian phase shift experienced by the TE pulse alone. The probe pulses are then injected into another PM fiber with a differential delay of $-2\Delta t$. The fast and slow axes of this PM fiber are orthogonal to those of the first section, resulting in a reversal of the delay between TE and TM pulses so that the TE pulse is now Δt ahead of the TM pulse. The control pulse B is then introduced between the TE and TM probe pulses before entering SOA2 where now the induced π radian phase shift affects only the TM pulse. The third PM fiber, with differential delay, Δt , recombines the TE and TM probe pulses in time. A π radian phase shift between

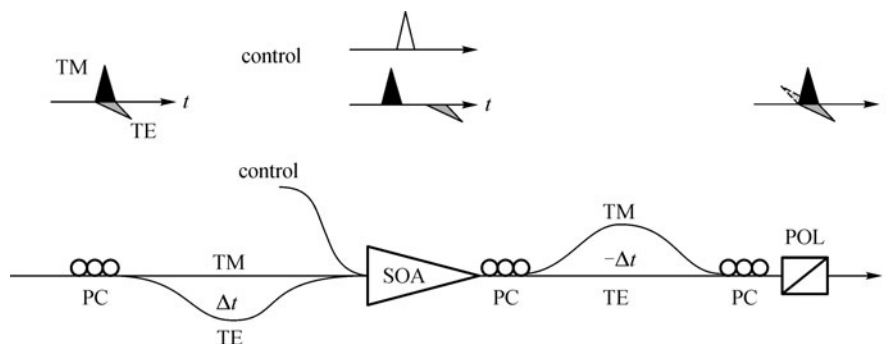


Fig. 1 Schematic setup of SOA-based UNI

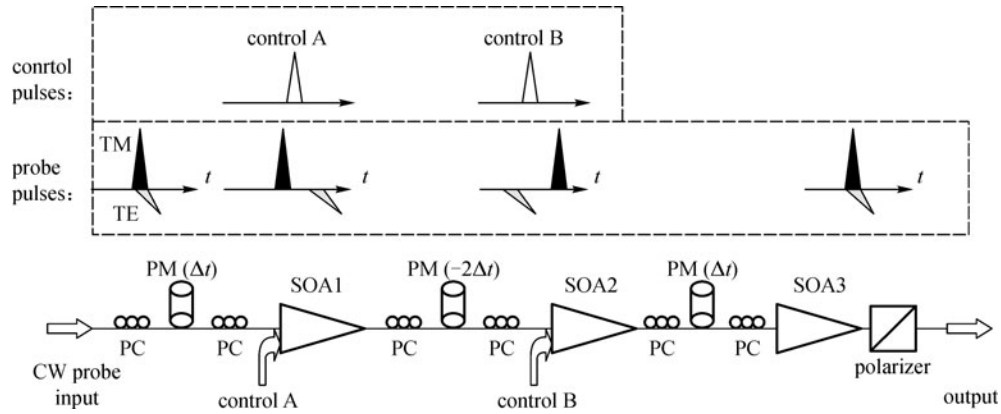


Fig. 2 Principle of dual-UNI XOR logic gate (PM: polarization maintaining fiber; PC: polarization controller)

TE and TM pulses gives a polarization rotation of $\pi/2$ when they recombine at the polarizer, which is crossed with respect to the un-rotated probe.

When both of the data pulses A and B are present, the nonlinear phase difference between TE and TM will be zero (first π , then $-\pi$, the same result as the case when both A and B are absent). In the cases of either A or B being present, the phase shift will be π . The system is biased OFF (no output) in the absence of the control data pulses. A pulse is generated after the polarizer only when one of A and B is present. Hence, the device satisfies the XOR logic truth table as shown in Table 1.

As with the conventional UNI gate, the probe pulses may be replaced by a CW beam, in which case the output takes the form of pulses of width Δt . Furthermore, when the probe pulse is a data stream A and the control data stream is data B, the output signal after SOA1-based UNI can be expressed as a Boolean function of $\overline{A}B$. Similarly, Boolean $A\overline{B}$ is obtained by injecting the probe data B and control data A in SOA2-based UNI. Due to the fact that an optical logic XOR gate can be expressed as $\overline{A}B + A\overline{B}$, therefore, by simply adding up two outputs from SOA1 and SOA2, the Boolean logic XOR functions can be obtained [5]. The corresponding XOR logic truth table is shown in Table 1.

Table 1 Logic truth table of $\overline{A}B$, $A\overline{B}$, and XOR

data A	data B	$\overline{A}B$	$A\overline{B}$	XOR
0	0	0	0	0
0	1	0	1	1
1	0	1	0	1
1	1	0	0	0

3 Experimental results of dual UNI 40-Gb/s XOR

A CW laser at the wavelength of 1580 nm is employed as

the probe beam in our case; therefore, the first PM fiber in Fig. 2 is not required. The experimental setup is shown in Fig. 3. The control pulses A and B are obtained from a 10.645-GHz mode-locked pulse laser source with center wavelength 1560 nm and pulse width 3 ps (full wave at half maximum (FWHM)). The control pulse stream is modulated with a $2^7 - 1$ pseudorandom bit sequence. The pulses are multiplexed to 42.58 Gb/s before injecting into the SOAs. An optical delay line is used to generate a different pattern for control pulses A and B. Variable optical attenuators (VOAs) are employed to change the control pulse energies. Another VOA is used to optimise the input power of the probe beam injected into SOA2.

The SOAs are both 1-mm long and have more than 30-dB small-signal gains at 400-mA bias current. They have a $1/e$ recovery time of ~ 25 ps. The differential delays of the PM fibers are ~ 23 ps ($2\Delta t$) and ~ 11.5 ps (Δt), respectively, where Δt is slightly less than one half of the bit period at the repetition rate of 42.58 GHz. Band-pass filters (BPFs) are used to block the control pulses and allow propagation of the probe beam. Each PM delay section includes polarization controllers (PCs) before and after the PM fiber. These permit the polarization of the probe beam to be appropriately aligned relative to the fast and slow axes of the PM fiber, and to the TE and TM modes of the SOA.

The output of the dual UNI is monitored by a 70-GHz oscilloscope. The 40-Gb/s XOR logic is shown in Fig. 4, which is in agreement with the function in Table 1. Note that the traces of data streams A and B of Fig. 3 are the outputs from the dual UNI, in the absence of B and A, respectively. The average powers of the probe CW beam are -5.7 and 1.9 dBm before SOA1 and SOA2, and the average powers of control pulses are 0.6 and 1.1 dBm, respectively. This implies that the control pulse energies are 57 and 64 fJ. The contrast ratio was obtained by comparing the average powers of ON and OFF states. More than 12 dB of the ER was observed.

The bit error rate (BER) measurements of the dual UNI

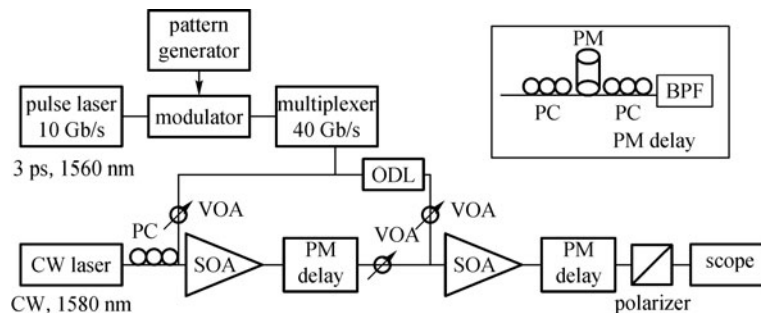


Fig. 3 Experimental set-up of 40-Gb/s XOR demonstration (PM delay is a set of PCs with a certain length of PM fiber; BPF: band-pass filter; VOA: variable optical attenuator; ODL: optical delay line)

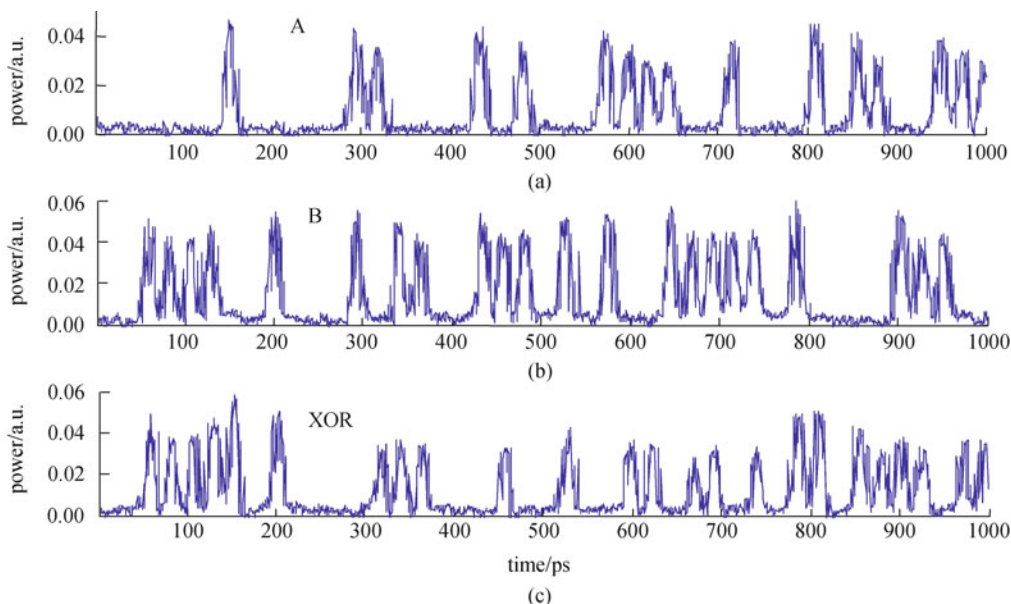


Fig. 4 Oscilloscope traces of 40-Gb/s XOR logic. (a) Output when data stream A only is ON; (b) output when data stream B only is ON; (c) XOR output (A and B ON)

are plotted in Fig. 5 [19]. Error-free XOR operation was realized, and no error floor was observed, with a power penalty of 5 dB at a BER of 10^{-9} compared with the back-to-back (B2B) signal. The eye diagram at 40 Gb/s is plotted as the insert in Fig. 5. The noise on the bottom level of the eye diagram originates from the filtered amplified spontaneous emission in the SOAs. There is additional noise on upper rail due to the patterning effect in the SOAs.

4 Experimental results of a simple 40-Gb/s XOR gate without probe beam

Another way to realize XOR gate is shown in Fig. 6, where A and B are served alternatively as probe and control data before SOA1 or SOA2. Two tunable mode-locked pulse lasers are used to generate 10.645 GHz, 3 ps (FWHM) pulses, with their central wavelengths at 1550 and 1560 nm. Polarization maintaining (PM) fibers with

differential delay of 23.48 ps, polarization controllers (PCs) and polarizers (POL) were used in each arm after the lasers to obtain data sequences at 42.58 Gb/s. By adjusting the relative optical delays before the SOAs, two 42.58-Gb/s data patterns of periodic 0110 and 1100 were constructed. Optical 1×2 90:10 couplers were used to split the incoming beam into a weak probe data (10%) and a strong control data (90%) for both A and B before the SOAs. Optical delay lines ODL1 and ODL3 were used to synchronize the probe data A and control data B before they were recombined by a 50:50, 2×1 coupler and launched into SOA1. Similarly, ODL2 was used to synchronize the control data A and probe data B before SOA2. The UNI was composed of two PM fibers with the same differential delay of 11.5 ps, PCs and a POL. The PM fibers were placed individually before SOA1 and SOA2, while it was shared in the common optical path after the SOAs. Band-pass filters were used after SOAs to block the corresponding control data. Pulse patterns of input,

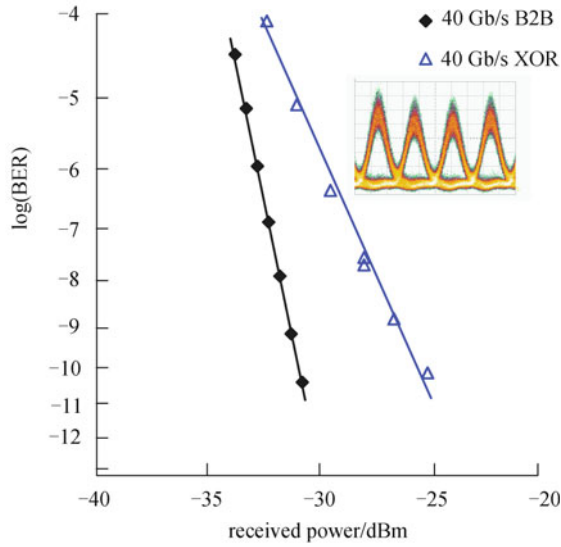


Fig. 5 BER of 42.6-Gb/s dual UNI logic (insert is corresponding eye diagram of XOR output; B2B: back-to-back)

intermediate and output at different positions of the setup are illustrated in Fig. 6.

To show the XOR logic, we can check, for example, the last bit in data A and B in Fig. 6, where the data A is logic “0” and the data B is logic “1”. Before SOA1, the probe data A is “0”, while the control data B is “1”; this combination gives the output of SOA1 to be “0” following the logic $A\bar{B}$. Similarly, before SOA2, the probe B is “1”, while the control A is “0”; therefore, the output of SOA2 is “1”, following $\bar{A}B$. Finally, the sum of these two signals gives “1”, which verifies the XOR operation of A and B. Figure 7 shows the traces of the input signals A and B, along with the output of Boolean $A\bar{B}$, $\bar{A}B$, and XOR logic functions, recorded by a 70-GHz oscilloscope using optical

to electrical conversion by a 40-GHz photodiode. As shown in Fig. 7, the XOR logic function is verified for all four different combinations of data inputs (“1” and “0”), as listed in Table 1. In the setup, commercially available SOAs were used, with a small-signal gain of 30 dB when the driving current was 300 mA. The average powers of the probe and control beam before SOA1 were -15.4 and -1.8 dBm, respectively. Similarly, the average powers of the probe and control beam before SOA2 were -17.8 and -9.3 dBm, respectively. Accordingly, the switching control pulse energies were 33 and 6 fJ for SOA1 and SOA2, respectively. The ER of the XOR gate was estimated to be 10 dB. It should be mentioned that the measured ER was under the condition of the deteriorated data signal A and B inputs after amplifying, filtering, and passing through delay lines; the ER can be further improved in the case of better quality of the input sequences A and B.

Compared to the previous 10-Gb/s gate in Ref. [5], the XOR logic operation speed is extended to 40 Gb/s using SOA-based UNI configuration, where XPM is employed instead of XGM to avoid the limitation of SOA carrier lift time. An exceptional case for XGM-based switching gate operating at a bit rate beyond 40 Gb/s can be expected using quantum-dot SOAs [20]; however, this kind of SOA is far away from practical implementation and out of the scope of this paper. Though this type of XOR gate is demonstrated at 40 Gb/s, it is expected to be operated beyond 40 Gb/s since SOA-based AND gate has been demonstrated successfully > 100 Gb/s [9,21]; further investigation on higher bit-rate operation of this gate is under way. Moreover, it is possible to make a hybrid integration version of the gate by carefully setting the delay and filtering in waveguides. Another improvement of this configuration is that the probe data and control data are launched at the same facet of the SOA (co-propagation), which avoids potential bit-rate restriction induced by the counter-propagation case, where the next pulse has to wait

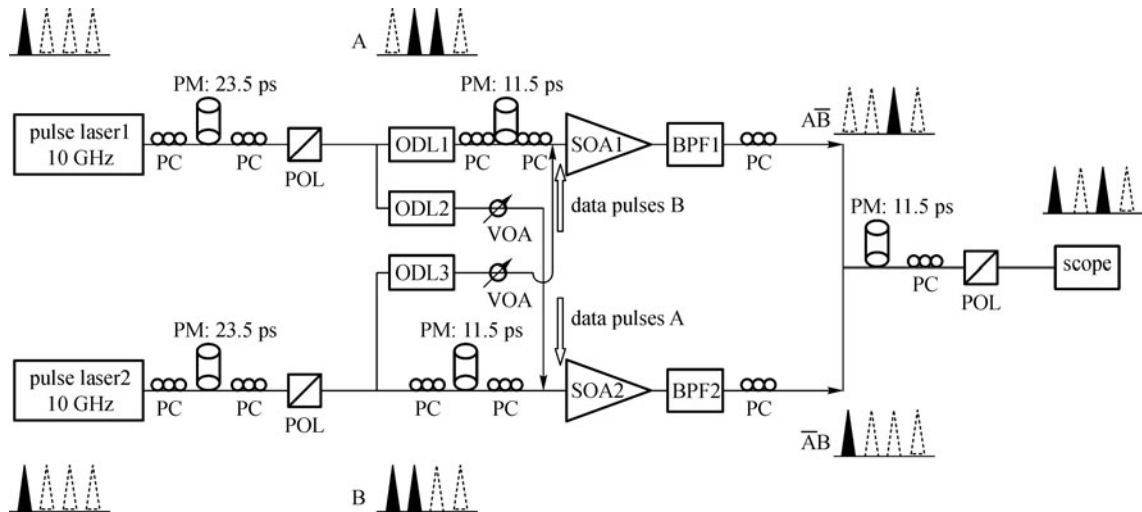


Fig. 6 Experimental setup of 40-Gb/s all-optical XOR gate

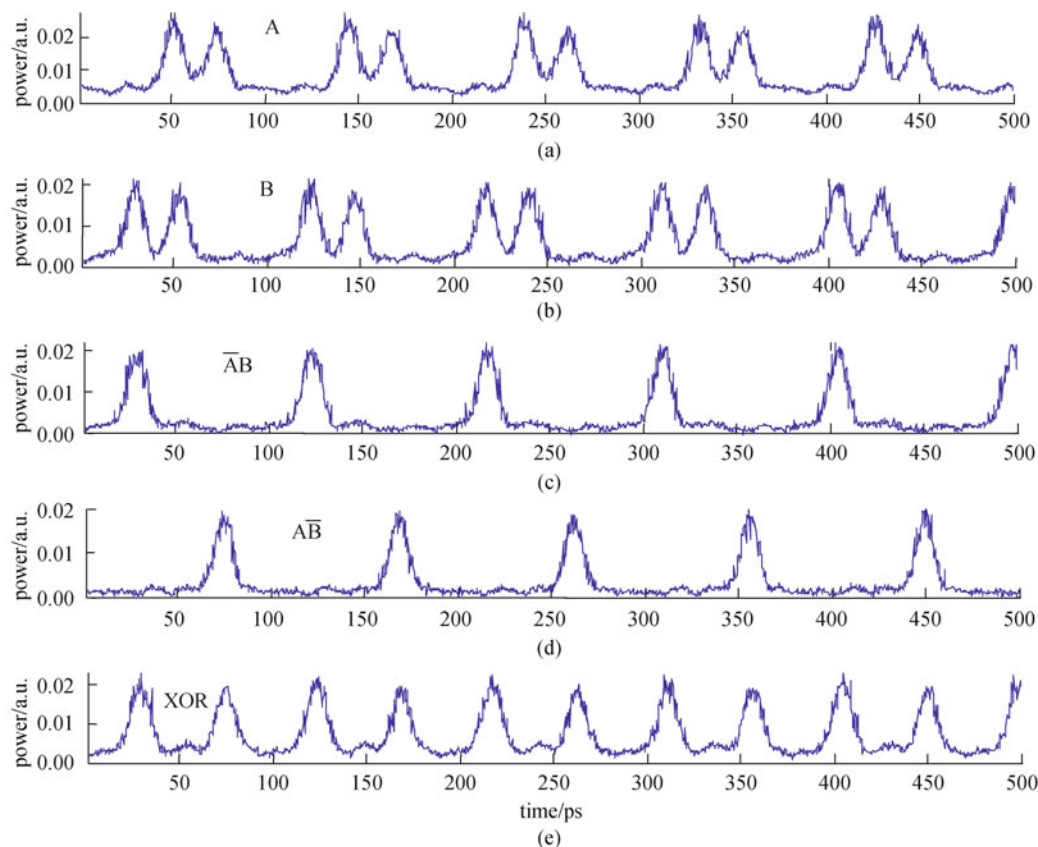


Fig. 7 Oscilloscopic traces of logic function of 40-Gb/s all-optical XOR gate corresponding to input data A and B (logic functions \overline{AB} and $A\overline{B}$ are also presented as intermediate stages). (a) A is ON; (b) B is ON; (c) \overline{AB} is ON; (d) $A\overline{B}$ is ON; (e) XOR is ON

until the previous pulse traveling through the full length of the SOA. For instance, assuming the effective refractive index of the SOA is 3, the SOA length has to be shorter than 1.25 mm for 40-Gb/s data in counter-propagation.

5 Experimental results of 85-Gb/s XOR

The transmission of control pulse A is blocked by a filter (not shown) placed before SOA2. SOA1 and SOA2 are, therefore, configured as a turbo-switch [17], and the effective switching speed by control pulse A is enhanced. The addition of a third SOA (also after a filter) to the original dual UNI forms a second turbo-switch that similarly enhances the speed of switching by control pulse B.

A CW laser with a wavelength of 1552 nm was employed as the probe beam instead of a pulse train, so the first PM fiber in Fig. 1 was not required. The experimental set-up is shown in Fig. 8. The 3-ps, 1557-nm control pulses A and B were obtained from a 10.645-GHz mode-locked laser. The control pulse stream was optically modulated with a $2^7 - 1$ PRBS, and the pulses were passively multiplexed to 85 Gb/s before being

injected into SOA1 and SOA2. An optical delay line was used to present different parts of the sequence to each SOA. Two VOAs were employed to adjust the control pulse energies. Another VOA was used to optimise the input power of the probe beam injected to SOA2.

All the three (Kamelian) SOAs were biased at 400 mA, where their unsaturated gain was greater than 30 dB. The differential delays of PM fibers were 11.5 ps ($2\Delta t$) and 5.75 ps (Δt), respectively, where Δt is one half of the bit period at 85 Gb/s. 5-nm band-pass filters blocked the control pulses and allowed the propagation of the probe beam. The PCs in front of each PM fiber were adjusted to launch approximately equal amplitudes into the TE and TM modes. The two polarization states were also aligned with the TE and TM modes of the active layer at the input to SOA1 and SOA2 with further PCs. This was to prevent the control pulses causing polarization rotation.

The output of the XOR logic gate was monitored by a 70-GHz oscilloscope. XOR operation was realized at 10, 21, 42, and 85 Gb/s by adjusting the control pulse multiplexer. The amplitude variations in the 85-Gb/s output eye diagram (Fig. 9) were primarily due to imperfections in the multiplexer. The output spectrum at the same rate is shown in Fig. 10, where the sidebands are

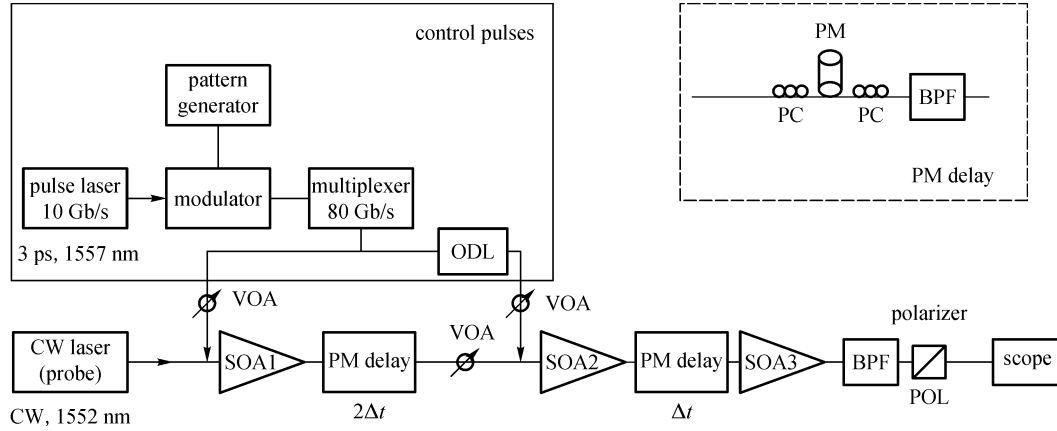


Fig. 8 Experimental 85-Gb/s XOR logic gate (PM delay indicates a length of PM fiber with PCs and a filter (inset))

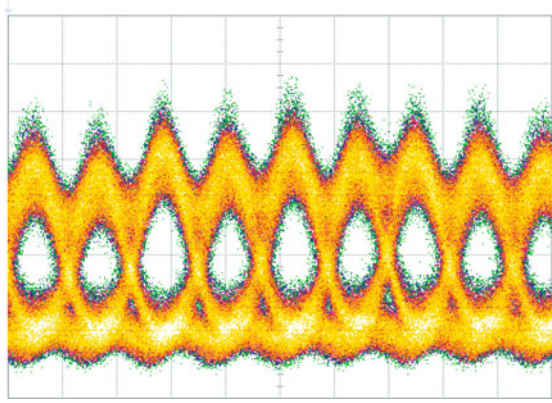


Fig. 9 85-Gb/s XOR output eye diagram (5 ps/division)

visible but suppressed compared to a normal return-to-zero AND gate spectrum (inset of Fig. 10). This is because the output pulses resulting from an $A\bar{B}$ input are in anti-phase

to those corresponding to $\bar{A}B$. The average power of the probe beam was 4 dBm before SOA1 and SOA2, and 10 dBm before SOA3. The average powers of control pulses A and B were 4 and 3.5 dBm, respectively, implying control pulse energies of 54 and 62 fJ.

6 Discussion and conclusion

We have reviewed a few new all-optical XOR logic gates at 40–85 Gb/s, in which the SOAs switch at the bit rate, not twice the bit rate as in the previously reported push-pull topology [12], providing the potential for higher ultimate operating speed. Given that single UNI-based AND gates have been operated at up to 160 Gb/s [9], we have successfully demonstrated XOR logic operation of the dual UNI at 40 Gb/s. The control pulse energies needed for switching at 40 Gb/s are 57 and 64 fJ, and the contrast ratio of the XOR output is > 12 dB.

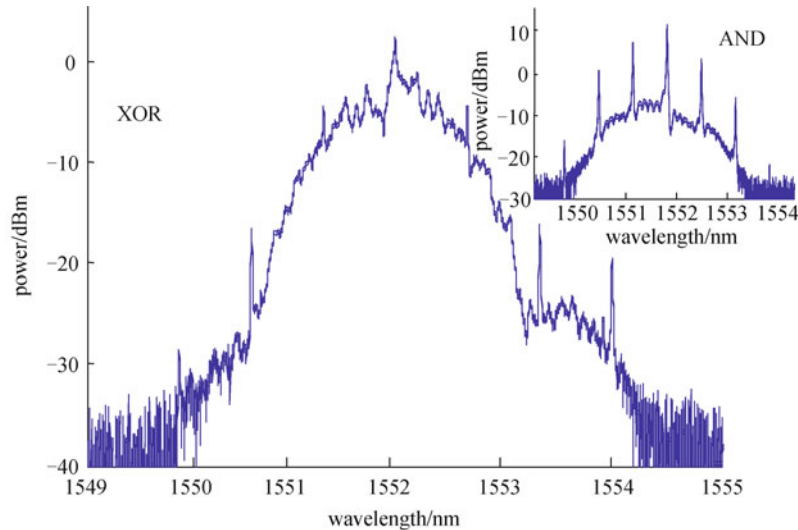


Fig. 10 Spectrum of 85-Gb/s XOR output (resolution is 0.01 nm; inset is corresponding spectrum of an 85-Gb/s AND gate)

A simple 40-Gb/s all-optical XOR gate is also demonstrated, where the inputs are only two data streams (A and B), while no additional probe beam is required. SOA-based UNI is employed as the switching element using XPM in SOA, which ensures the XOR gate operation at 40 Gb/s or beyond. The switching energies of the XOR gate are as low as 6–33 fJ/pulse.

Finally, we have proposed and demonstrated for the first time an all-optical 85-Gb/s XOR logic gate based on SOAs. A substantial speed improvement has been obtained by adding a third SOA to the dual UNI configuration in order to benefit from the turbo-switch effect. The control pulse energies needed for switching were 54 and 62 fJ.

Acknowledgements This work was supported by the Science Foundation Ireland, the National Nature Science Foundation of China, and the State Key Laboratory of Advanced Optical Communication Systems and Networks, Shanghai Jiao Tong University.

References

1. Cotter D, Manning R J, Blow K J, Ellis A D, Kelly A E, Nesses D, Phillips I D, Poustie A J, Rogers D C. Nonlinear optics for high-speed digital information processing. *Science*, 1999, 286(5444): 1523–1528
2. Manning R J, Ellis A D, Poustie A J, Blow K J. Semiconductor laser amplifiers for ultrafast all-optical signal processing. *Journal of the Optical Society of America B*, 1997, 14(11): 3204–3216
3. Webb R P, Yang X, Manning R J, Maxwell G D, Poustie A J, Lardenois S, Cotter D. All-optical binary pattern recognition at 42 Gb/s. *Journal of Lightwave Technology*, 2009, 27(13): 2240–2245
4. Patel N S, Hall K L, Rauschenbach K A. 40-Gbit/s cascaded all-optical logic with an ultrafast nonlinear interferometer. *Optics Letters*, 1996, 21(18): 1466–1468
5. Kim J H, Jhon Y M, Byun Y T, Lee S, Woo D H, Kim S H. All-optical XOR gate using semiconductor optical amplifiers without additional input beam. *IEEE Photonics Technology Letters*, 2002, 14(10): 1436–1438
6. Sartorius B, Bornholdt C, Slovak J, Schlak M, Schmidt C, Marculescu A, Vorreau P, Tsadka S, Freude W, Leuthold J. All-optical DPSK wavelength converter based on MZI with integrated SOAs and phase shifters. In: *Proceedings of Optical Fiber Communication Conference 2006*. 2006, OWS6
7. Kang I, Dorner C, Zhang L, Rasras M, Buhl L, Bhardwaj A, Cabot S, Dinu M, Liu X, Cappuzzo M, Gomez L, Wong-Foy A, Chen Y F, Patel S, Neilson D T, Jaques J, Giles C R. Regenerative all optical wavelength conversion of 40 Gb/s DPSK signals using a semiconductor optical amplifier Mach-Zehnder interferometer. In: *Proceedings of the 31st European Conference on Optical Communications (ECOC 2005)*. 2005, Th4.3.3
8. Ueno Y, Nakamura S, Tajima K, Kitamura S. 3.8-THz wavelength conversion of picosecond pulses using a semiconductor delayed-interference signal-wavelength converter (DISC). *IEEE Photonics Technology Letters*, 1998, 10(3): 346–348
9. Nakamura S, Ueno Y, Tajima K. 168 Gb/s all-optical wavelength conversion with a symmetric Mach-Zehnder-type switch. *IEEE Photonics Technology Letters*, 2001, 13(10): 1091–1093
10. Ueno Y, Nakamura S, Tajima K. Nonlinear phase shifts induced by semiconductor optical amplifiers with control pulses at repetition frequencies in the 40–160-GHz range for use in ultrahigh-speed all-optical signal processing. *Journal of the Optical Society of America B*, 2006, 19(11): 2573–2589
11. Wang Q, Zhu G, Chen H, Jaques J, Leuthold J, Piccirilli A B, Dutta N K. Study of all-optical XOR using Mach-Zehnder interferometer and differential scheme. *IEEE Journal of Quantum Electronics*, 2004, 40(6): 703–710
12. Webb R P, Manning R J, Maxwell G D, Poustie A J. 40 Gbit/s all-optical XOR gate based on hybrid-integrated Mach-Zehnder interferometer. *Electronics Letters*, 2003, 39(1): 79–81
13. Webb R P, Yang X, Manning R J, Giller R. All-optical 40 Gb/s logic XOR gate with dual ultrafast nonlinear interferometers. In: *Proceedings of the 31st European Conference on Optical Communications (ECOC 2005)*. 2005, Tu3.5.1
14. Webb R P, Yang X, Manning R J, Giller R. All-optical 40 Gbit/s XOR gate with dual ultrafast nonlinear interferometer. *Electronics Letters*, 2005, 41(25): 1396–1397
15. Yang X, Manning R J, Hu W. Simple 40 Gbit/s all-optical XOR gate. *Electronics Letters*, 2010, 46(3): 222–223
16. Yang X, Manning R J, Webb R P. All-optical 85 Gb/s XOR using dual ultrafast nonlinear interferometer and turbo-switch configuration. In: *Proceedings of the 32nd European Conference on Optical Communications (ECOC 2006)*. 2006, Th1.4.2
17. Manning R J, Yang X, Webb R P, Giller R, Garcia Gunning F C, Ellis A D. The ‘turbo-switch’—a novel technique to increase the high-speed response of SOAs for wavelength conversion. In: *Proceedings of Optical Fiber Communication Conference 2006*. 2006, OWS8
18. Kang I, Rasras M, Buhl L, Dinu M, Cabot S, Cappuzzo M, Gomez L T, Chen Y F, Patel S S, Dutta N, Piccirilli A, Jaques J, Giles C R. All-optical XOR and XNOR operations at 86.4 Gb/s using a pair of semiconductor optical amplifier Mach-Zehnder interferometers. *Optics Express*, 2009, 17(21): 19062–19066
19. Yang X, Mishra A K, Manning R J, Webb R P, Maxwell G, Poustie A J, Harmon B. Comparison of all-optical XOR gates at 42.6 Gbit/s. In: *Proceedings of the 33rd European Conference and Exhibition on Optical Communication (ECOC 2007)*. 2007, P070
20. Akiyama T, Ekawa M, Sugawara M, Sudo H, Kawaguchi K, Kuramata A, Ebe H, Morito K, Imai H, Arakawa Y. An ultra-wideband (120 nm) semiconductor optical amplifier having an extremely-high penalty-free output power of 23 dBm realized with quantum-dot active layers. In: *Proceedings of Optical Fiber Communication Conference 2004*. 2004, PDP-12
21. Hall K L, Rauschenbach K A. 100-Gbit/s bitwise logic. *Optics Letters*, 1998, 23(16): 1271–1273